

From Pulsar Spin to Pulsar Wind: The Spectral Connection?

E.V. Gotthelf and C.M. Olbert

Columbia Astrophysics Laboratory, Columbia University, 550 West 120th Street, New York, NY 10027

Abstract. We present preliminary results from a systematic spectral study of pulsars and their wind nebulae using the *Chandra X-Ray Observatory*. The superb spatial resolution of *Chandra* allows us to differentiate the compact object’s spectrum from that of its surrounding nebulae. Specifically, for six Crab-like pulsars, we compare spectral fits of the averaged pulsar wind nebulae (PWN) emission to that of the central core using an absorbed power-law model. These results suggest an empirical relationship between the bulk averaged photon indices for the PWNe and the pulsar cores; $\Gamma_{PWN} = 0.8 \times \Gamma_{Core} + 0.8$. The photon indices of PWNe are found to fall in the range of $1.3 < \Gamma_{PWN} < 2.3$. We propose that the morphological and spectral characteristics of the pulsars observed herein seem to indicate consistent emission mechanisms common to all young pulsars. We point out that the previous spectral results obtained for most X-ray pulsars are likely contaminated by PWN emission.

1. Introduction

Recent observation of pulsars associated with supernova remnants obtained with the *Chandra X-ray* observatory (Weisskopf, O’Dell & van Speybroeck 1996) are providing an unprecedentedly detailed view of pulsar wind nebulae. For the first time, emission features involving wisps, co-aligned toroidal structures, and axial jets are fully resolved in X-rays on arc-second scales. These features, similar to those seen from the optical Crab nebula, are now found to be common to young, energetic pulsar in supernova remnants (Gotthelf 2001). Herein we present preliminary spectral analysis of several PWNe observed with *Chandra*, which, collectively, suggest a fundamental observational relationship between the spectral characteristics of pulsars and their pulsar wind nebulae.

Table 1 presents spectral results from a sample of *Chandra* pulsars which have characteristic wind nebulae. A summary of these objects along with references and images can be found in Gotthelf (2001). All observations were obtained with the ACIS-CCD camera which is sensitive to X-rays in the 0.2–10 keV band with an energy resolution

of $\Delta E/E \sim 0.1$ at 1 keV. The on-axis point spread function is slightly undersampled by the CCD pixels (0.5”) allowing us to isolate the pulsar emission from that of the nebula. Except for N157B, which serendipitously fell on ACIS-I0, all data were obtained with ACIS-S3. The data were collected in nominal spectral (“FAINT”) and timing (3.24 s) mode and reduced and analyzed using the latest version of CIAO (CIAO 2.2/CALDB v.2.9). Starting with the Level 1 processed event files we corrected the event data for CTI effects (Townsend et al. 2001) and applied the standard Level 2 filtering criteria, then further rejected time intervals of anomalous background rates.

For each object listed in Table 1, we extracted spectra from the PWN, pulsar core, and background, when available, or obtained spectral parameters from the literature as indicated. For the core spectra, the brightest central pixels were extracted based upon data above 4.0 keV, where the core emission is substantially greater than that of the surrounding nebula. The nebula itself was then extracted from the region above which the background was constant, excluding the core. Large variations in background rates and size of both the nebula and the central source amongst observations precluded the use of a standard extraction aperture. Custom spectral response matrix functions (RMFs) were provided with the CTI correction software, and ancillary response functions (ARFs) were created according to standard CIAO 2.2 procedures, using the QEU calibration files similarly provided. All spectra were grouped to a minimum of 50 counts per spectral bin.

We fit the resultant background-subtracted pulsar and PWN spectra with a power-law model above 2 keV using the latest version of XSPEC (v11.1). The spectral fits to the core included a convolution model to account for pileup effects on the spectra. Table 1 lists the spectral parameters obtained for each object; the values for the Crab and N157B have been obtained from the literature (Willingale et al. (2001), Wang & Gotthelf 1998, respectively). No measurement of the pulsed spectrum for 3C58 is currently available. Absorption values were obtained by fitting the nebula spectra with an absorbed power-law above 0.6 keV, and were subsequently frozen for all future fits.

Table 1. Spectral Properties of Pulsars and their Wind Nebulae^a

Remnant	$\Gamma_{\text{PWN}}^{\text{Averaged}}$	Γ_{Core}^b	Γ_{Pulsed}^c	$\log L_{\text{x NS}}$	$\log L_{\text{x PWN}}$
G11.2 – 0.3	1.28 ± 0.15	0.63 ± 0.12	0.60 ± 0.60	33.9	34.2
Vela XYZ	1.50 ± 0.04	0.95 ± 0.24	0.93 ± 0.26	31.2	32.6
Kes 75	1.88 ± 0.04	1.13 ± 0.11	1.10 ± 0.30	35.2	36.0
3C 58	1.92 ± 0.11	1.73 ± 0.15	...	33.0	...
Crab Nebula	2.11 ± 0.05	1.63 ± 0.09	1.86 ± 0.07	35.9	37.3
N157B Nebula	2.28 ± 0.12	2.07 ± 0.21	1.60 ± 0.35	35.9	36.1

^a Ranked by increasing **averaged** PWN photon index.

^b The value for the Crab pulsar has been obtained from the literature (Willingale et al. 2001). The measured photon-indices have been corrected for pile-up as discussed in the text.

^c Pulsed PI value references: Vela: Strickman, Harding & Jager (1999); G11.2-0.3: Torii et al. (1997); Kes 75: Gotthelf et al. (2000); Crab: Pravdo, Angelini & Harding (1997); N157B: Marshall et al. (1998).

The best-fit linear relationship between core and PWN photon indices is shown in Figure 1. We expect that the linear relationship seen in Fig. 1 may steepen slightly as we more fully account for pileup effects in the spectra. We note that the pileup corrected photon indices are likely subject to change due to the preliminary nature of the pileup model implementation, and suggest caution until these issues are resolved, but expect the basic result to remain unchanged.

We also note that due to extreme pileup effects and the brightness of its nebulae compared to the brightness of its core, SNR 0540-69 has not been included pending a more detailed analysis of the available data.

As a check to our final spectral results and to look for any systematic effect due to pile-up, we compare our measured power-law indices with those obtained from the literature for the pulsed emission for each source (Figure 2). Although they need not be the same, it is reassuring that they agree to within measurement errors.

2. Results

The photon indices obtained from this analysis show a trend that the average PWNe photon indices are consistently steeper than their core’s photon indices by a factor of one-half to one. We suggest that this relationship is linear, with the form $\Gamma_{\text{PWN}} = 0.8 \times \Gamma_{\text{Core}} + 0.8$. This trend may be due to a number of factors. It may imply that the synchrotron spectrum frequency break occurs close to the neutron star, that there is a fundamental difference in emission mechanisms between the two regions, or that the nebula is being powered by the core and that the steepening is due to synchrotron burn-off or a comparable aging mechanism.

Though pulsations have not yet been discovered in the nebulae in supernova remnants G21.5-0.9 and G54.1+0.3, we note that their spectral indices are in the range pre-

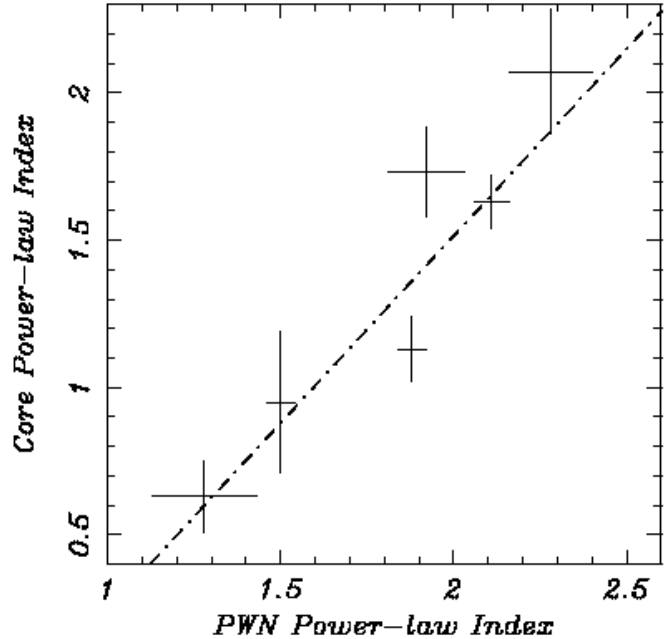


Fig. 1. $\Gamma_{\text{PWN}}^{\text{Averaged}}$ vs. Γ_{Core} – A plot of the power-law photon indices of the average pulsar wind nebulae spectra versus the pileup-corrected core photon indices for the collection of objects presented in Table 1. A dashed-line indicates the best-fit linear regression (i.e. $\Gamma_{\text{PWN}} = 0.8 \times \Gamma_{\text{Core}} + 0.8$). The physical origin of this relationship is yet to be determined.

dicted by this formula (Slane et al. 2000, Lu et al. 2002, respectively).

Chandra is the first telescope able to spatially resolve the neutron star from the nebula. Previous spectral observations of pulsars are likely to be strongly contaminated by PWN emission. For example, we see no clear relationship between the power-law spectral index obtained for these pulsars by *ASCA* with any of those measured by *Chan-*

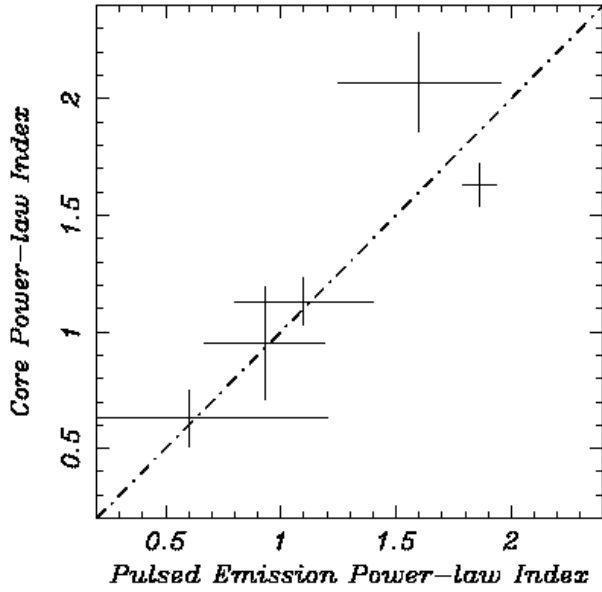


Fig. 2. $\Gamma_{\text{Core}}^{\text{Pulsed}}$ vs. Γ_{Core} – A comparison between the subset of measured power-law photon index for the core emission of objects presented in Table 1 and the pulsed emission for each of these source obtained from the literature (from ASCA or XTE fits). A one-to-one correspondence is indicated by the dashed line.

dra. As more crab-like pulsars are observed and analyzed, a more complete picture of their morphological and spectral characteristics comes into view, paving the way for future models and simulations.

Acknowledgements. We gratefully acknowledge the support by the Heraeus foundation. This work made possible by NASA LTSA grant NAG 5-7935. C.M.O. also acknowledges the support of the I.I. Rabi Scholars Program at Columbia University.

References

- Gotthelf, E. V., Vasisht, G., Boylan-Kolchin, M., et al. 2000, ApJL, 542, L37
- Gotthelf, E. V. 2001, Proc. The 20th Texas Symposium on Relativistic Astrophysics, AIP Press; astro-ph/0105128
- Lu, F. J., Wang, Q. D., Aschenbach, B., Durouchoux, P., & Song, L. M. 2002, ApJL, 568, L49
- Marshall, F. E., Gotthelf, E. V., Zhang, W., et al. 1998, ApJL, 499, L179
- Pravdo, S. H., Angelini, L., & Harding, A. K. 1997, ApJ, 491, 808
- Slane, P., Chen, Y., Schulz, N. S., Seward, F. D., Hughes, J. P., & Gaensler, B. M. 2000, ApJL, 533, L29
- Torii, K., Tsunemi, H., Dotani, T., & Mitsuda, K. 1997, ApJL, 489, L145
- Townsley, L. K., Broos, P. S., Garmire, G. P., Nousek, J. A., ApJL, 534, L139
- Strickman, M. S., Harding, A. K., & de Jager, O. C. 1999, ApJ, 524, 373
- Wang, Q. D. & Gotthelf, E. V. 1998, ApJL, 509, L109

- Weisskopf, M. C. O'Dell, S. L., van Speybroeck, L. P. 1996, Proc. SPIE 2805, Multilayer and Grazing Incidence X-ray/EUV Optics III, 2
- Willingale, R., Aschenbach, B., Griffiths, R. G., et al. 2001, A&A, 365, L212